Combined and Hybrid Geothermal Power Systems

14

Ronald DiPippo
Renewable Energy Consultant, Dartmouth, MA, United States

14.1 Introduction and Definitions

This chapter discusses integrated power plant systems that consist of various geothermal energy conversion systems or a geothermal plant combined with a plant using at least one other source of energy. The former are called "combined systems" and the latter "hybrid systems." In all cases the objective of combining plant types is to achieve synergy, meaning that the integrated system is capable of performance superior to that of individual plants. This may mean higher utilization or thermal efficiency, more net power, or a better economic outcome. Combined geothermal systems may consist of various flash-steam units or binary plants in an integrated combination that achieves advantages and benefits not realizable in separate units.

A hybrid geothermal-natural gas power plant for The Geysers geothermal field in California, USA, was proposed and considered in 1984 [1]. Among the first attempts to conceptualize and analyze hybrid geothermal power plants was carried out at Brown University in the late 1970s and early 1980s [2–11]. A commercial proposal that stemmed from one of the Brown studies concerned a geothermal-coal power plant at Roosevelt Hot Springs, Utah, that would have supplied electricity to the City of Burbank, California; it went through a thorough engineering verification before being shelved in favor of a conventional coal plant [12], despite indications of significant advantages. The equations presented here draw upon the studies by the Brown research group. Another concept was put forth by Hiriart and Gutierrez in 1995 and involved the use of solar superheating of separated steam at Cerro Prieto, Mexico [13]. These and several more recent projects are described in this chapter.

Since there are many options available to measure the performance of an integrated plant, equations are developed to provide the basis to assess the synergistic characteristics of these designs. First, basic thermodynamic principles are applied to this situation (Section 14.2), followed by theoretical integrated designs involving various flash-steam units (Section 14.3) and ones that combine flash-steam units with binary units (Section 14.4). Next geothermal and fossil energy resources are integrated to form hybrid plants of differing designs (Section 14.5), followed by plants that combine geothermal and solar energy resources (Section 14.6). Nuclear,

Geothermal Power Generation. https://doi.org/10.1016/B978-0-443-24750-7.00017-8

hydroelectric and wind power plants do not lend themselves to hybrid designs with geothermal plants. As appropriate throughout, examples of plants either in operation or that have been subjected to extensive research or feasibility studies are described in some detail.

14.2 General Thermodynamic Considerations

Fig. 14.1 depicts the general scheme of a power system involving three different sources of primary energy. Geothermal, fossil, and solar energy are selected for this illustration. The stand-alone, state-of-the-art (SOTA) geothermal, fossil fuel, and solar plants are denoted by G, F, and S, respectively. As shown, each plant receives input energy, produces work output, and discharges waste energy. In the figure and equations that follow, asterisks emphasize that the three plants represent the best that can be achieved by each one given the current technology. The hybrid plant, H, receives the same energy inputs as the three separate plants and produces work while rejecting some waste energy.

The energy terms may be heat transfer in cases where this is the appropriate form of input, but they should generally be the exergy delivered to and rejected from each plant. This allows various types of energy to be placed on the same thermodynamic footing. Thus, using exergy allows for a valid comparison of heat obtained from burning fossil fuels, hot pressurized geofluids used either directly as in flash plants or indirectly in binary plants, and radiant solar energy used either directly as in photovoltaics (PVs) or indirectly as in concentrating solar power (CSP) thermal plants. Here it is assumed that the analyses of all these individual systems are well known and may be conducted based on established techniques.

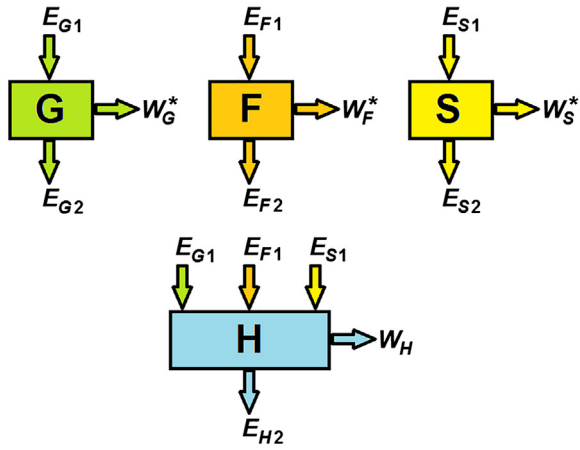

Figure 14.1 Schematic depiction of individual geothermal, fossil, solar, and hybrid plants. *F*, fossil; *G*, geothermal; *H*, hybrid; *S*, solar.

Several metrics are available to assess the worth of the hybrid system; see Eqs. (14.1)–(14.4). First, an overall assessment is made by calculating the overall hybrid figure of merit, F_H, which is achieved by comparing the output of the hybrid plant with the sum of the outputs of the individual SOTA plants, that is,

$$F_H = \frac{W_H}{W_G^* + W_F^* + W_S^*}. \tag{14.1}$$

Obviously, for the hybrid plant to hold a thermodynamic advantage over separate plants, $F_H > 1$. It is also of interest to find figures of merit for individual sources of energy. Thus, geothermal, fossil fuel, and solar figures of merit for the hybrid plant may be defined as follows:

$$F_G = \frac{W_H - \left(W_F^* + W_S^*\right)}{W_G^*} \tag{14.2}$$

$$F_F = \frac{W_H - \left(W_S^* + W_G^*\right)}{W_F^*} \tag{14.3}$$

$$F_S = \frac{W_H - \left(W_G^* + W_F^*\right)}{W_S^*}. \tag{14.4}$$

Defined this way, each of the three equations attributes to each energy source, respectively, all the synergistic power gains from the hybrid plant by debiting the hybrid output by the maximum obtainable from the other two sources using SOTA power plants.

Other useful measures of the efficacy of hybrid plants exist but are beyond the scope of this chapter; the reader may consult Refs. [4–8].

SOTA outputs may be estimated using a utilization efficiency, η_u, for each type of energy input, where the efficiency gives the fraction of the supplied "fuel" exergy that can be converted into useful output. Thus, one arrives at Eqs. (14.5)–(14.7):

$$W_G^* = \eta_{uG}\, E_{G1} \tag{14.5}$$

$$W_F^* = \eta_{uF}\, E_{F1} \tag{14.6}$$

$$W_S^* = \eta_{uS}\, E_{S1}. \tag{14.7}$$

By using individual SOTA plants, a high bar is set for hybrid designs. They may be established based on the best available plants for the types of energy being considered. For example, a SOTA plant might be a dual-reheat, supercritical-pressure coal-fired plant with seven feedwater heaters, natural-gas-fired aeroderivative gas turbine, triple-flash geothermal steam plant, dual-pressure hot water geothermal binary plant, parabolic-trough or power tower CSP plant, or high-efficiency PV plant.

Representative values for utilization efficiencies depend on the nature and characteristics of the "fuel" and plant design. For example, a SOTA geothermal binary plant may exhibit η_u values ranging from 10%−16% for resource temperatures ranging from about 120−165°C, whereas flash-steam plants may have values from 35%−55% for single-, double-, or triple-flash designs. Coal plants have values from 35%−45% depending on the steam pressure, number of reheats, and number of feedwater heaters. Simple gas-fired turbine plants may approach values of up to 40%, whereas CSP plants may be limited to about 30%. PV solar plants generally can convert about 10%−15% of incident solar energy to electrical output. The highest conversion efficiency among fossil fuel plants, 60%, is achieved using gas turbine and steam turbine combined cycles. However, these plants are themselves combined systems and might not be an appropriate comparison for assessing geothermal hybrid systems.

Considerations besides thermodynamics also bear on the suitability of a hybrid plant. For example, the environmental impacts must not be worse than individual plants and preferably should be better. A reasonable method must be in place to absorb waste energy from the plant. Permits must be obtained for not just one type of energy usage but for each one in a hybrid plant. Even a highly efficient power plant will not be built unless the economics are favorable, permits are obtainable, an offtaker is found to purchase the electricity, and funding can be arranged.

Central to the matter of economics is the relative proximity of the different energy sources. Fossil fuels can be mined or obtained by drilling and then moved to the location of the power plant, whereas geothermal "fuels" must be used very near their source. Solar energy is available anywhere albeit in different strengths and for different time durations. The geothermal energy component therefore determines where the hybrid plant must be built. Typically, solar energy will be available at the site in some form, but fossil fuel may be problematic. However, except in the case of mine-mouth coal plants, the fuel will need to be shipped or piped somewhere for exploitation in a power plant. Certainly, natural gas is almost always sent by pipeline to power stations. So a site-specific economic analysis is critical to determining the efficacy of using fossil fuel in a conventional plant or shipping it to a geothermal site instead.

Thus, thermodynamics, the focus of this chapter, provides a necessary but not sufficient outcome concerning the superiority and acceptance of any hybrid or combined power plant.

14.3 Combined Single- and Double-Flash Systems

Geothermal field development often occurs in discrete stages, starting with small wellhead units and progressing to simple single-flash plants and then possibly to combined single- and double-flash plants. Fig. 14.2 shows a combined single- and double-flash power station comprising two single-flash units and one double-flash unit. The synergy is obvious in this case. Since all the waste brine from the first two units is used as the input for the third, the combined plant will generate more power than the two single-flash units. If the units were operated on a stand-alone basis, the geofluid needed for the

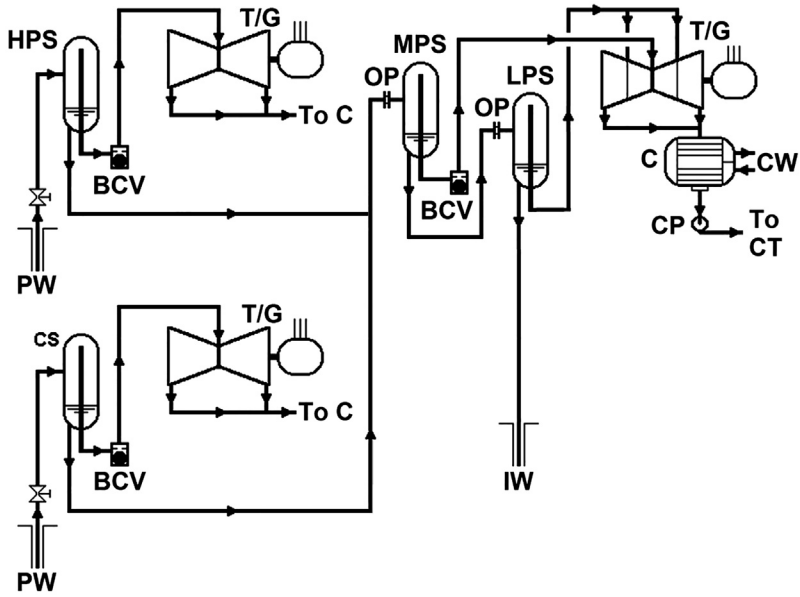

Figure 14.2 Combined single- and double-flash plant; see Nomenclature.

double-flash unit would have to be obtained from new wells drilled purposely for that unit. That extra geofluid would mean more exergy would need to be extracted from the reservoir for power equivalent to that produced by the combined system.

An example of this type of plant used to exist at the Cerro Prieto I power station in Baja California, Mexico. Originally, four single-flash units of 37.5 MW each were constructed. The waste brine was disposed of in a large evaporation pond. As soon as confidence was established in the longevity of the resource, a fifth unit was constructed to put all the waste brine to use in the manner shown in Fig. 14.2. Two lower-pressure steam flows were created by flash and separation processes to drive a dual-pressure, dual-admission turbine that added 30 MW more power without the need to drill more wells. Thus, a 20% amplification of power output and utilization efficiency was achieved.

A similar result was obtained at Ahuachapán in El Salvador when a third, double-flash unit was added to two existing single-flash units. The original power capacity of 60 MW (2×30 MW) was increased to 95 MW with the 35 MW low-pressure unit, a 58% amplification that was achieved by flashing the brine from wellhead separators and using other low-pressure wells that could not be used with the original units.

14.4 Combined Flash and Binary Systems

Many fields begin their operating lives with a single-flash unit until confidence in the field justifies additional units. One common way to extend the output of the initial unit

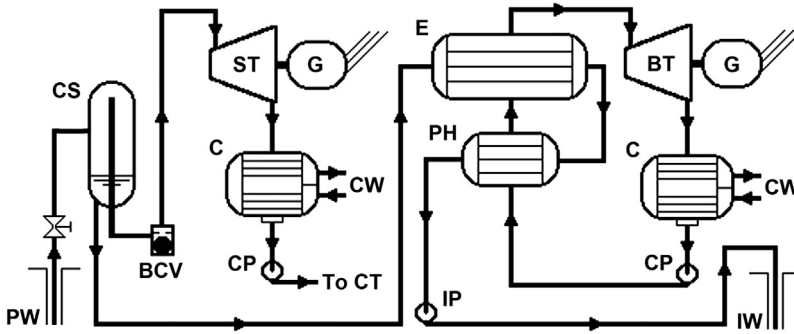

Figure 14.3 Combined flash-binary power plant; see Nomenclature.

is to add a bottoming binary unit that capitalizes on the waste geofluid that is typically reinjected from the first unit. This option creates a combined flash-binary plant and is an alternative to the combined flash plant described in Sect. 14.3. As in that case, the synergy is obvious as additional power can be generated from the same amount of geofluid being extracted from the reservoir. A flow diagram for such a system is shown in Fig. 14.3.

There are numerous examples of this arrangement. For example, Unit 5 at Miravalles in Costa Rica, where a pair of binary cycles capitalize on the roughly 900 kg/s of 165°C separated brine coming from three single-flash units, adding some 15 MW to the 137 MW from the flash units, and raising the utilization efficiency of the whole operation by about 13% with no additional wells [14]. Similar designs are found at Brady's Hot Springs, Beowawe, Steamboat Hills, and Dixie Valley, all of which are flash plants with bottoming binary cycles in the state of Nevada, USA.

A further advantage of this arrangement is that chemical scaling can be better controlled using a binary bottoming cycle than a bottoming flash plant. Flashing the waste brine raises the concentration of minerals in the brine, such as silica, but merely cooling the brine as in a binary plant keeps the concentration of minerals constant, and thereby allows more cooling than would be possible in the flash case. It is still possible to over-cool the brine, but the saturation point is at a lower temperature than with a flash plant. This can be an important consideration in many geothermal fields.

An alternative design to the combined flash-binary system shown in Fig. 14.3 is the integrated flash-binary plant shown in Fig. 14.4. This type of plant is designed as a unit and installed as a single plant. It is particularly appropriate for high-temperature resources in areas of environmental sensitivity where emissions of any kind are to be avoided. One distinguishing feature of this plant is that all the geofluid extracted from the reservoir is reinjected. This includes even the noncondensable gases (NCGs) released from the pressurized liquid brine as the geofluid passes through the plant equipment. In this design, NCGs are captured from the steam at the evaporator of the upper binary cycle, compressed, delivered to the waste brine holding tank, returned to solution, and finally reinjected along with the waste brine.

Plants of this general design are in operation at: Puna, Hawaii, USA; Amatitlán, Guatemala; and Rotokawa and Ngatamariki, New Zealand, and elsewhere.

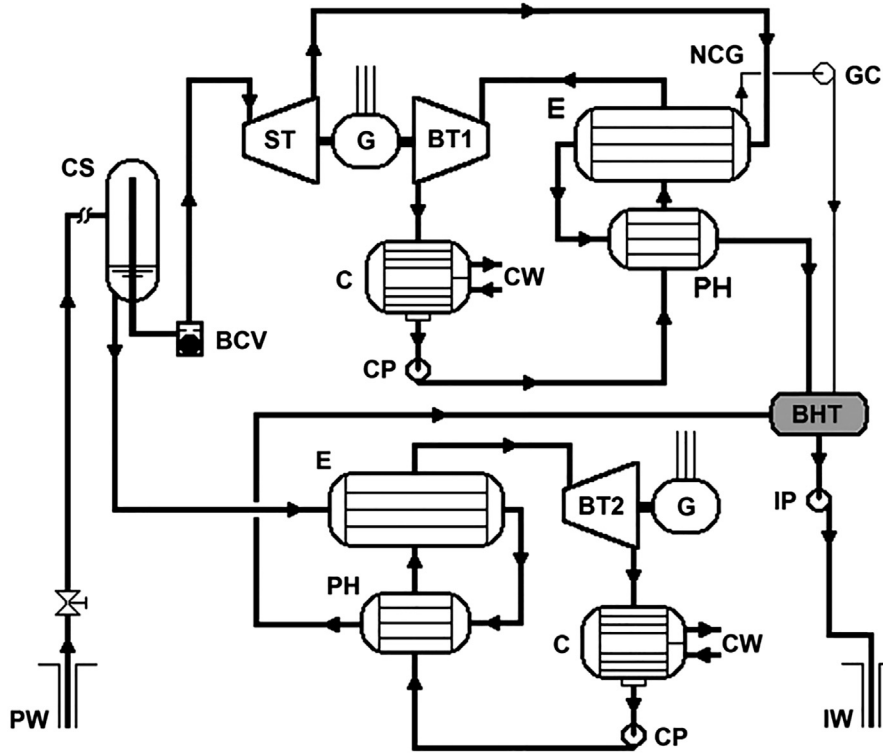

Figure 14.4 Integrated two-level flash-binary power plant; see Nomenclature.

14.5 Geothermal–Fossil Hybrid Systems

Geothermal and fossil energy resources lend themselves to hybrid configurations, presuming the resources are colocated or the transportation costs to bring the fossil fuel to the geothermal site are acceptable. Many design options are available depending on the nature of the fossil fuels.

14.5.1 Fossil-Fueled Superheated Geothermal Steam Plants

Using fossil fuels to enhance geothermal resources was proposed as long ago as 1924 by Caufourier [2]. His idea was to pass saturated steam obtained by several stages of flashing hot water from natural springs through a furnace fired with coal to obtain superheated steam that then drove a multistage steam turbine to make electricity; see Fig. 14.5. It is not known if this idea was ever brought to fruition, but a simple assessment showed that it would have had about 65% utilization efficiency [15].

A similar proposal was made to superheat the geothermal steam at the dry steam power plant at The Geysers in 1984 by employing a natural gas supply that was handy to the site [16]. There were two schemes; the first would operate with gas-fired heaters,

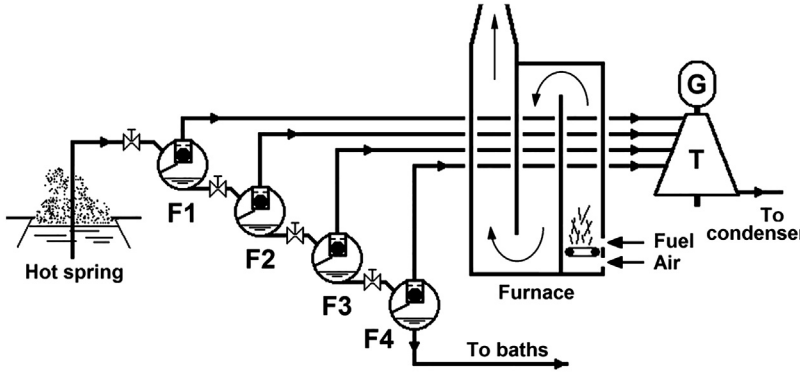

Figure 14.5 Multistage geothermal steam plant with fossil superheating [2,15]; see Nomenclature.

while the other would involve constructing a gas turbine unit with the exhaust heat supplying the geothermal steam superheating, much like the now common combined steam and gas turbine plants. Neither proposal was ever built even though the utilization of both the fossil and geothermal "fuels" would have been greatly improved.

In general, any geothermal resource may be enhanced through superheating. Fig. 14.6 shows such a system built on a geothermal double-flash plant; by eliminating the flash vessel and the low-pressure turbine (LPT), the system becomes a single-flash with superheat.

A parametric study of the plant in Fig. 14.6 [5] showed that for geofluid inlet temperatures in a range of 175−250°C and 540°C superheat temperature, this system has an overall figure of merit F_H ranging from 1.05 to 1.075, a geothermal F_G ranging from 1.06 to 1.10 and a fossil-fuel F_F ranging from 1.20 to 1.34.

A study conducted for this chapter considered an optimized double-flash plant receiving geofluid from a 245°C reservoir with a condenser operating at 52°C and a fossil-fired superheater added along with a recuperator, as shown in Fig. 14.6.

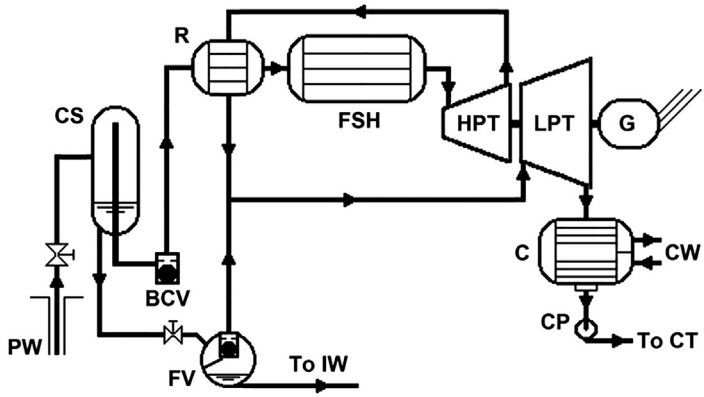

Figure 14.6 Double-flash geothermal plant with fossil superheating; see Nomenclature.

Steam and water properties were obtained from NIST REFPROP software [17] that was embedded into an Excel spreadsheet written to analyze the plant. The stand-alone double-flash plant produced 111.2 kW per kg/s of geofluid from the production well. Assuming a dead state at 30°C, this gives a utilization efficiency of 44.9%. The superheater raises the geosteam temperature leaving the recuperator from 283.5 to 540°C, considered to be the metallurgical limit. The hybrid plant produces 151.5 kW per kg/s, an increase of 36.2%. The input exergy of the heat added in the superheater is found by assuming it could be used in an ideal power cycle between the average temperature of the combustion gases and the dead-state temperature. Thus, the total exergy input to the hybrid plant comes to 288.8 kW per kg/s, giving a utilization efficiency of 52.5%. The processes are shown in a scale temperature−entropy diagram; see Fig. 14.7. Pressure losses in piping and heat

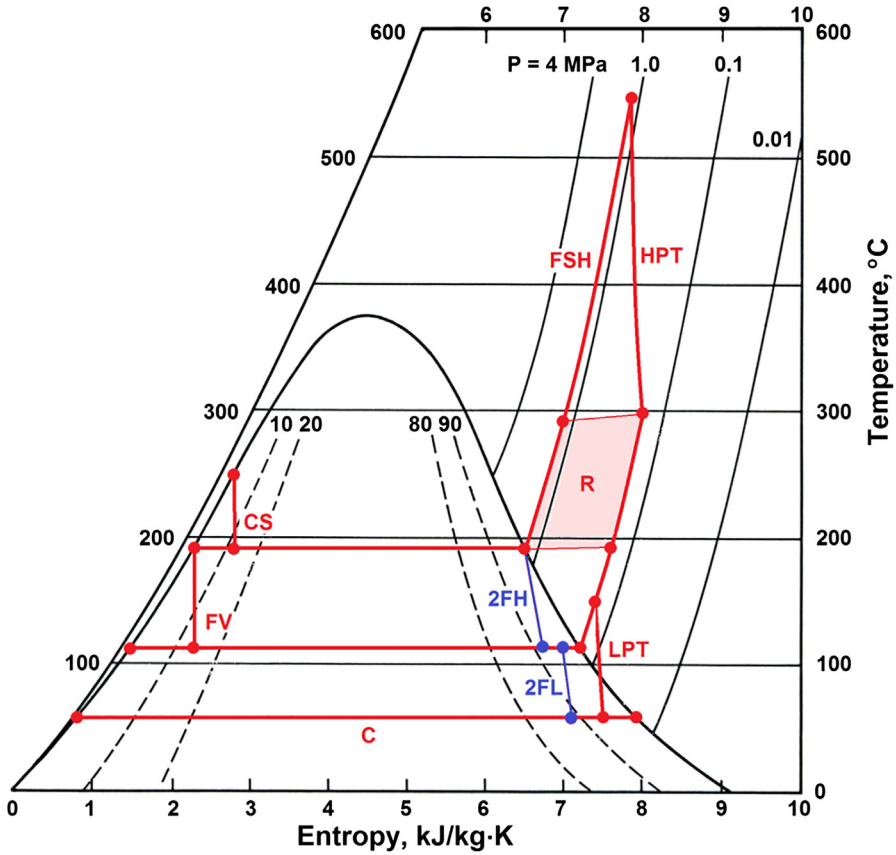

Figure 14.7 Temperature−entropy process diagram (to scale) for example cited. Process labels correspond to Fig. 14.6; turbine processes 2FH and 2FL are for the basic double-flash plant, both of which are replaced by the HPT and LPT of the hybrid system. See Nomenclature for abbreviations.

exchangers were ignored, but wet turbine efficiencies were calculated from the Baumann rule to account for performance degradation caused by moisture [15].

14.5.2 Coal-Fired Plants With Geothermal-Heated Feedwater

Whereas the previous system was a geothermal plant with an assist from fossil fuel, the system described in this section is the opposite, that is, a fairly conventional fossil fuel, typically coal-fired, central power station with a geothermal assist. Fig. 14.8 shows a simplified schematic of a typical arrangement.

The geothermal fluid provides some of the heating of the feedwater, eliminating some or all of the low-pressure feedwater heaters normally placed between the condensate pump (CP) and the deaerator (DA) that require steam from the LPT to affect the heating. This allows the use of lower-temperature geofluids that could not be used effectively in a geothermal power plant, while allowing more power to be generated by the fossil plant owing to higher steam mass flow through the lower-pressure stages of the turbine.

A systematic parametric study [4] of a geothermal preheat hybrid system built on a standard subcritical fossil-fueled central station found that over a geofluid temperature range from 150 to 250°C the overall F_H ranged from about 1.02 to 1.05, the fossil F_F

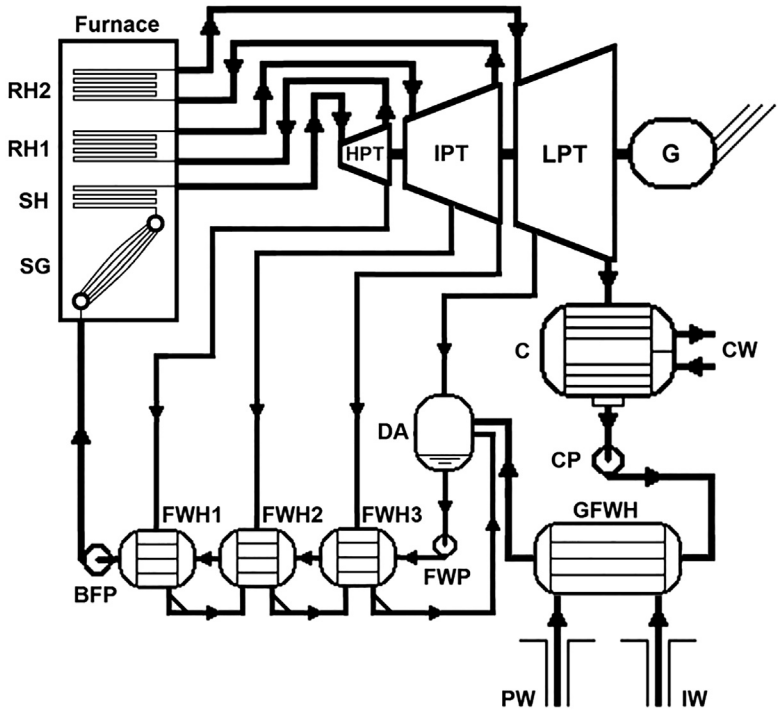

Figure 14.8 Geothermal preheat system; see Nomenclature.

ranged from about 1.02 to 1.06, and the geothermal F_G ranged from 1.50 to 1.44. The same study using a supercritical fossil plant showed nearly identical F_H and F_F as the subcritical case, but the F_G ranged from 1.71 to 1.55 over the same temperature range.

An engineering proposal for a 750 MW hybrid coal-geothermal power plant of the geothermal-preheat type was put forth by the city of Burbank, California, in the late 1970s. Several assessments were conducted [18] for a plant to be sited at Roosevelt Hot Springs, Utah, and the conclusions were as follows:

- A well-designed hybrid plant could generate electricity at a lower cost than either a conventional SOTA coal plant or a SOTA geothermal plant.
- Geothermal energy would contribute more than 20% of the energy input to the hybrid plant.
- The hybrid plant would use geothermal energy far more efficiently than any conceivable all-geothermal plant. For high-grade geothermal resources, the hybrid plant would have a 20% higher utilization efficiency; for low-grade resources, the improvement would be a 150%−200% improvement.

A further study by the Ralph M. Parsons engineering firm verified the technical and economic feasibility of the hybrid power plant [19]. In spite of the advantages held by the hybrid design, a conventional coal-fired plant, the 2 × 950 MW Intermountain Power Plant, was built instead.

14.5.3 Compound Hybrid Geothermal−Fossil Plants

It is possible to combine the two previous hybrid systems to form a compound hybrid plant, as shown in Fig. 14.9. The plant uses a single-flash geothermal unit that derives

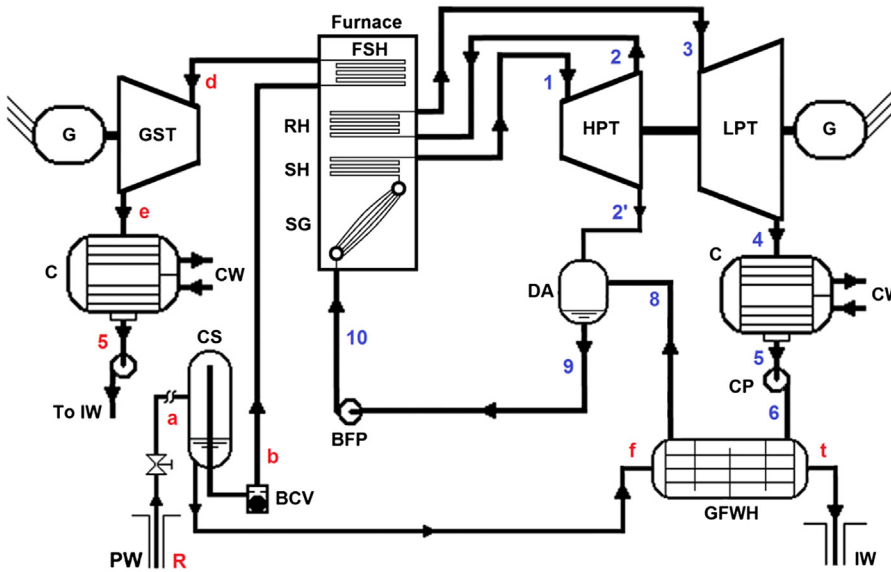

Figure 14.9 Compound fossil−geothermal hybrid plant. Note: State points are keyed to Fig. 14.10; see Nomenclature.

superheat from the furnace of a conventional fossil-fired central plant while providing a portion of the feedwater heating to the fossil plant by means of the hot separated geothermal brine. A double-flash geothermal plant may also be used in a similar manner but with more complexity [6,9].

With reference to Fig. 14.9, there are several adjustable parameters that define the operating pattern of such a plant. The mass fraction of steam entering the cyclone separator (CS) is fixed by the reservoir geofluid condition and the wellhead pressure, the latter being a degree of freedom in the design. Likewise, the steam temperature entering both fossil turbines, the high-pressure turbine (HPT) and the LPT, can be specified along with their pressures. The fraction of steam extracted from the HPT to feed the deaerator (DA) may be set so as to produce a saturated liquid entering the boiler feed pump (BFP). Both condensers may be assumed to operate at the same pressure (vacuum) since both are supplied with cooling water from a cooling tower. The geothermal feedwater heater (GFWH) can be designed for a certain terminal temperature difference (TTD), and this allows the determination of the geothermal-to-pure-water mass flow ratio. The three turbines, including the geothermal steam turbine (GST), will operate essentially as dry expanders and may be characterized by typical isentropic efficiencies.

A study was performed for this chapter using the following assumptions:

Geofluid production mass flow rate = 100 kg/s.
Geothermal wellhead temperature = 200°C.
Geothermal quality (dryness fraction) at inlet to CS = 0.20.
HPT and LPT inlet temperatures = 540°C.
HPT and LPT inlet pressures = 16.5 and 4.0 MPa, respectively.
GST inlet temperature = 510°C.
Condensing pressure = 0.0056 MPa.
GFWH TTD = 10°C.
HPT isentropic efficiency = 0.82.
LPT and GST isentropic efficiency = 0.85.
CP and BFP isentropic efficiency = 0.80.
Pressure and heat losses were ignored.

Table 14.1 shows the properties at the state points; Table 14.2 gives the main results. The efficiency of the plant may be measured in several ways. The overall thermal efficiency based on the total heat added from the fossil fuel is 53.0%. Looking only at the pure steam side of the plant, the thermal efficiency is 48.0%, obtained by subtracting the output of the GST from the total net power and dividing by only the heat input to the pure water and steam from the fossil fuel. The synergy created by combining the simple fossil-fuel plant with the single-flash geothermal plant with the geothermal brine heater (BH) and the fossil-fired geothermal steam superheater allows the plant to gain nearly 5% points of efficiency, which is about a 10% improvement.

A full parametric analysis was carried out in Ref. [6] for a system defined in Fig. 14.9 for three values of wellhead temperature, four values of wellhead quality (or dryness fraction), and including 10% pressure losses in all piping and heat exchangers. Each combination of wellhead temperature and dryness fraction corresponds to a different reservoir temperature. The results for the overall hybrid, fossil, and

Table 14.1 State-point properties for compound hybrid plant shown in Fig. 14.9

State	T	P	s	h	x	$\dot{m}$
	C	MPa	kJ/kgK	kJ/kg		kg/s
1	540.00	16.5	6.4298	3406.45	SH	91.79
2	341.95	4	6.5516	3073.08	SH	91.79
2′	341.95	4	6.5516	3073.08		11.30
3	540.00	4.000	7.2075	3537.47	SH	80.49
4	34.91	0.0056	7.8532	2410.27	0.9363	80.49
5	34.91	0.0056	0.5039	146.24	0.0000	80.49
6	35.25	4	0.5071	151.26	CL	80.49
8	190.00	4	2.2315	808.69	CL	80.49
9	250.35	4	2.7968	1087.49	0.0000	91.79
10	254.36	16.5	2.8041	1106.95	CL	91.79
res	269.37	5.45	2.9708	1240.22	0.0000	**100**
a	200.00	1.55	3.1505	1240.22	0.2000	**100**
b	200.00	1.55	6.4302	2792.01	1.0000	20
d	510	1.555	7.5828	3495.00	SH	20
e	34.91	0.0056	8.1515	2502.15	0.9743	20
f	200.00	1.55	2.3305	852.27	0.0000	80
t	45.25	1.555	0.6412	190.83	CL	80

Table 14.2 Performance of compound hybrid plant shown in Fig. 14.9

Heat Input to Steam Generator (SG)	211,069 kWt
Heat input to reheater (RH)	37,378 kWt
Heat input to geosteam superheater (FSH)	14,060 kWt
Total heat input	262,507 kWt
Power output from HPT	30,600 kWe
Power output from LPT	90,727 kWe
Power output from GST	19,857 kWe
Total turbine power output	141,183 kWe
CP power required	404 kWe
BFP power required	1786 kWe
Total pump power required	2190 kWe
Net plant power output	138,993 kWe

geothermal figures of merit are shown in Table 14.3. The F_G values are impressive, while the F_H and F_F values are less so, but in all cases, synergy exists in the hybrid arrangement.

14.5.4 Gas Turbine Topped–Geothermal Flash-Steam Hybrid Plant with Superheating

Patterned after the highly efficient combined steam and gas turbine power plants, the gas turbine topping cycle with a geothermal flash plant makes for an interesting hybrid

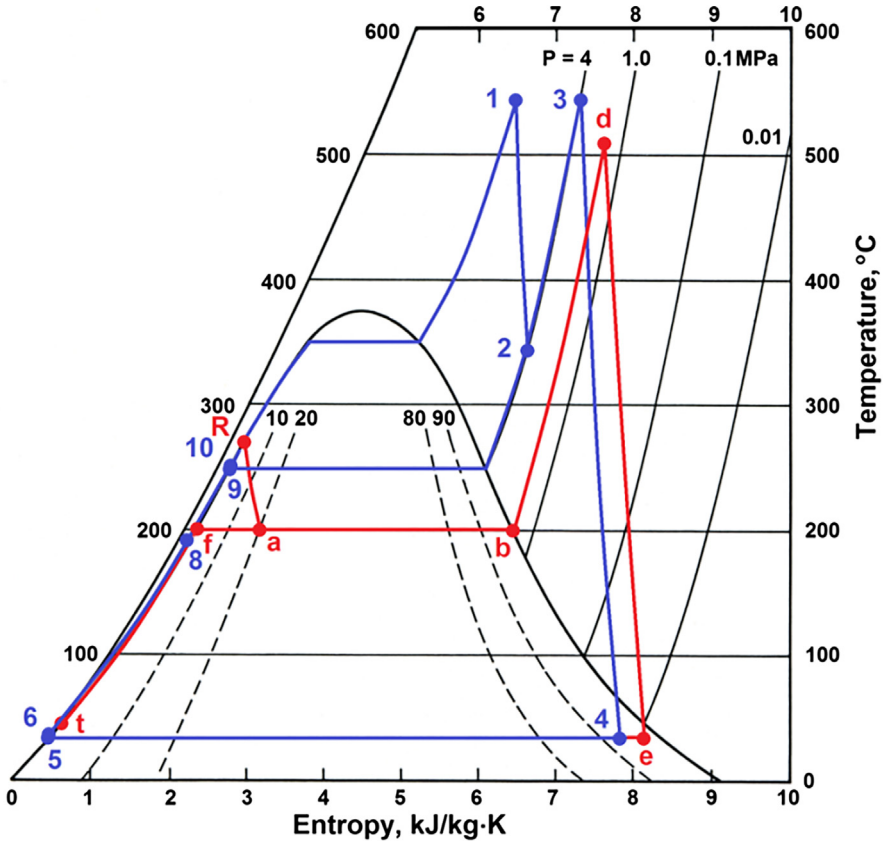

Figure 14.10 Temperature−entropy process diagram for hybrid plant shown in Fig. 14.9. State 5 applies to both pure water and geothermal steam condensate; states 5 and 6, and states 9 and 10 are indistinguishable on this diagram.

Table 14.3 Figures of merit for compound hybrid plants with single-flash [6]

Wellhead temperature (°C)	FM	Wellhead dryness fraction			
		0.10	0.20	0.30	0.40
150	F_H	1.032	1.045	1.059	1.074
	F_F	1.034	1.048	1.066	1.087
	F_G	1.612	1.562	1.535	1.517
200	F_H	1.066	1.083	1.102	1.123
	F_F	1.072	1.094	1.121	1.153
	F_G	1.759	1.696	1.657	1.631
250	F_H	1.095	1.116	1.138	1.163
	F_F	1.109	1.139	1.174	1.216
	F_G	1.745	1.707	1.681	1.663

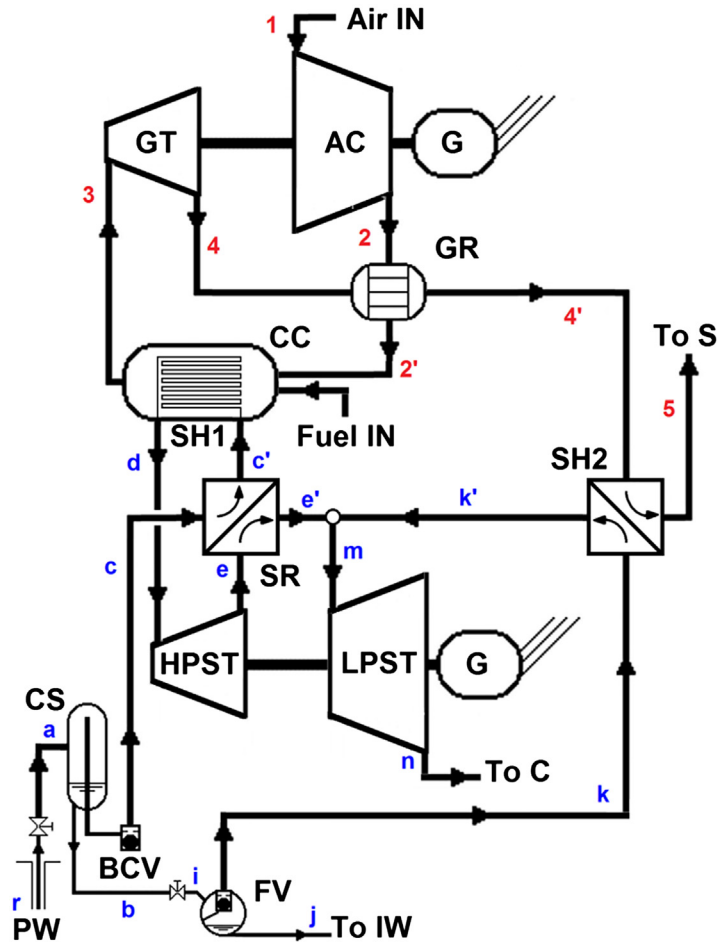

Figure 14.11 Gas turbine topped−geothermal double-flash hybrid system; see Nomenclature.

plant [3]. Fig. 14.11 shows a schematic arrangement of such a system. The geosteam from the cyclone separator (CS) first passes through a steam-side recuperator (SR) on its way to being superheated as part of the gas turbine combustion process (SH1). From the high-pressure steam turbine, the geosteam provides the initial heating of the separated steam in the SR and then mixes with the low-pressure flashed steam that has been superheated by the gas turbine exhaust (SH2). The merged streams then drive the low-pressure steam turbine. Other than allowing for the superheating of the separated geosteam, the gas turbine cycle is fairly standard.

The thermodynamic process diagrams are shown in Figs. 14.12 and 14.13 in scale-drawn temperature−entropy coordinates. They are not superimposed in a single diagram owing to the very high temperatures at which the gas turbine cycle operates. All heat transfer and work processes are depicted as arrows.

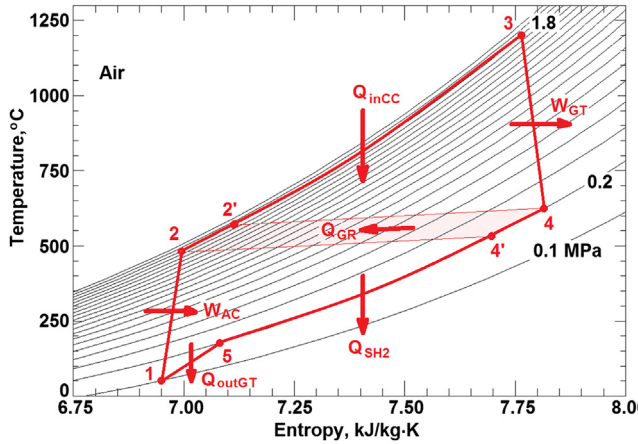

Figure 14.12 Temperature−entropy diagram for gas turbine processes for plant in Fig. 14.11.

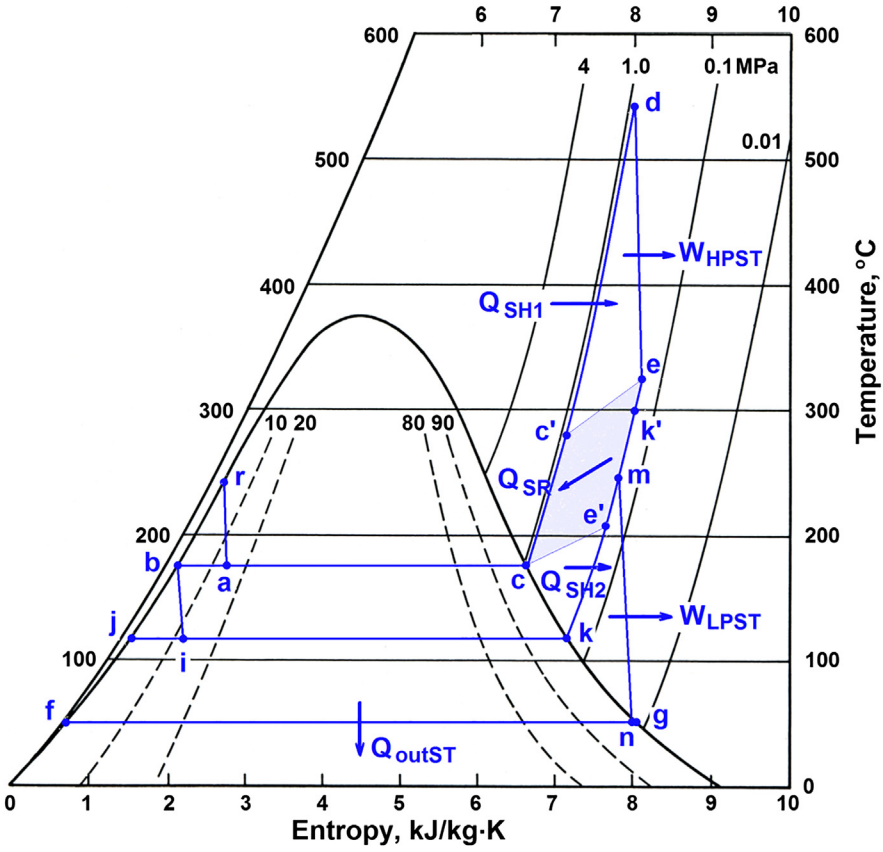

Figure 14.13 Temperature−entropy diagram for double-flash processes for plant in Fig. 14.11.

A set of representative state points were assigned and a system analysis carried out. This example is not optimized but illustrates the advantages that can be achieved with the hybrid system. Table 14.4 lists the temperature, pressure, enthalpy, and mass flow rates for an assumed 100 kg/s geofluid flow from the reservoir. The other fixed parameters are shown as **bold numbers** in the table. The following assumptions were made regarding component efficiencies: isentropic efficiency for the air compressor = 0.87, for the gas turbine = 0.92, and for both high- and low-pressure steam turbines = 0.85; in addition, the effectiveness of both the steam recuperator and the gas regenerator = 0.65. There was no need to deploy the Baumann rule for the steam turbines since both operated essentially completely dry, as shown in Fig. 14.13.

The summary of calculations is given in Table 14.5, indicating that the heat rejected from the gas turbine to the surroundings is very small, 1404 kWt, whereas

Table 14.4 State-point data for gas-turbine-topped geothermal-double-flash hybrid power plant

State	Description	T	P	h	$\dot{m}$
		°C	MPa	kJ/kg	kg/s
Gas turbine plant side					
1	Air compressor inlet	**35**	**0.1**	308.52	9.91
2	Air compressor outlet	472.78	1.8	763.90	9.91
2′	Gas regenerator HP outlet	577.92	1.8	879.68	9.91
3	Gas turbine inlet	**1200**	**1.8**	1605.70	9.91
4	Gas turbine outlet	634.34	**0.2**	942.02	9.91
4′	Gas regenerator LP outlet	530.19	0.2	826.24	9.91
5	Superheater 2 outlet	**175**	0.2	450.21	9.91
Geothermal plant side					
r	Reservoir geofluid	**240**	**3.8469**	1037.60	**100**
a	Cyclone separator inlet	**175**	0.8926	1037.60	100
b	Separated liquid outlet	175	0.8926	741.02	85.40
c	Separated vapor outlet	175	0.8926	2772.71	14.60
c′	Steam recuperator HP outlet	275.39	0.8926	3001.93	14.60
d	HP steam turbine inlet	**540**	0.8926	3567.23	14.60
e	HP steam turbine outlet	325.91	0.1692	3125.36	14.60
e′	Steam recuperator LP outlet	211.97	0.1692	2896.13	14.60
i	Flash vessel inlet	**115**	0.1692	741.02	85.40
j	Flash liquid outlet	115	0.1692	482.59	75.44
k	Flash vapor outlet	115	0.1692	2698.58	9.96
k′	Superheater 2 outlet	**300**	0.1692	3072.83	9.96
m	LP steam turbine inlet	247.79	0.1692	2967.80	24.56
n	LP steam turbine outlet	**50**	0.0124	2566.82	24.56
f	Condenser liquid outlet	**50**	0.0124	209.34	24.56
g	Condenser saturated vapor	**50**	0.0124	2591.29	—

Table 14.5 Summary of results for gas-turbine-topped geothermal-double-flash hybrid power plant

Heat transfer terms	
Rate of heat transfer in combustion chamber	7197 kWt
Rate of heat transfer in superheater 1	8252 kWt
Rate of total heat transfer from fossil fuel	15,449 kWt
Rate of heat transfer inside gas regenerator	1148 kWt
Rate of heat transfer inside steam recuperator	3346 kWt
Rate of heat transfer inside superheater 2	3727 kWt
Rate of heat transfer out of gas turbine cycle	1405 kWt
Rate of heat transfer out of double-flash plant	57,893 kWt
Electrical power terms	
Power output of gas turbine	6579 kWe
Power consumption of air compressor	4514 kWe
Net power developed by gas turbine plant	2065 kWe
Power output of HP steam turbine	6450 kWe
Power output of LP steam turbine	9847 kWe
Total power of steam turbines	16,297 kWe
Total power of hybrid plant	18,362 kWe
Exergy input terms	
Exergy input to gas turbine from heat input in CC	5618 kW
Exergy input to steam from heat input in SH1	4973 kW
Total exergy input from fossil fuel	10,591 kW
Exergy input from geofluid (reservoir state)	21,435 kW
Total exergy input to hybrid plant	32,025 kW
Efficiency terms	
Thermal efficiency of gas turbine plant	0.2869
Utilization efficiency of gas turbine plant	0.3675
Utilization efficiency of hybrid plant	0.5734
Pure double-flash plant	
Power output of HP steam turbine	3477 kW
Power output of LP steam turbine	7430 kW
Total power of steam turbines	10,906 kW
Utilization efficiency of pure double-flash plant	0.5088

the heat rejected from the steam plant is very large, 57,893 kWt. This is a consequence of the internal heat transfer within the gas regenerator (GR) and from the GT plant to the 2-flash plant (SH2). The very high heat rejection per unit of power generated in the geothermal plant is typical of such plants and leads to large cooling towers to absorb the waste heat. Also shown are the exergy inputs to the hybrid plant. Each heat transfer term has an associated exergy found by assuming the heat transfer is used in an ideal Carnot cycle between the highest temperature at which the heat is received and the dead-state temperature (35°C). Thus, the exergy

equals the heat transfer value multiplied by the Carnot efficiency, namely, $1 - (T_0 / T_H)$. The thermal efficiency for the GT part of the plant is about 29%, whereas the utilization efficiency is about 37%; the utilization of the hybrid plant is over 57%. This may be compared with 51% utilization efficiency for a pure double-flash plant.

Thus, the hybrid power plant holds a 12% utilization efficiency advantage over a simple geothermal double-flash plant with no superheating, and a 54% advantage over the gas turbine plant with a heat regenerator. These are important gains for the hybrid system and demonstrate high synergy with this arrangement.

14.5.5 Geothermal–Biomass Hybrid Plants

Many geothermal power stations are situated where agricultural or forestry operations exist, creating a supply of vegetation or wood waste that can be considered fuel for a geothermal-biomass plant. For example, some plants in Larderello, Italy are being upgraded with biomass. A pair of dry steam plants at Cornia, 2×20 MW, have been redesigned to accommodate a biomass furnace to superheat the geothermal steam. One of the plants has been shut down for several years and will serve as the location for the furnace, while the other plant, only 150 m away, will serve as the power generator. A simplified schematic of the system is shown in Fig. 14.14.

The plant is fed steam from two well areas: Area 1 provides dry, slightly superheated steam at 210°C, while Area 2 yields 2-phase geofluid at the wellhead at 156°C and about an 18% dryness fraction. The two streams are mixed at a pressure of 0.55 MPa and fed to the biomass superheater where the temperature is raised to 370°C. The combined mass flow is 30.6 kg/s and produces about 19.2 MW from the turbine, assuming equal steam flows from the two well areas; originally the turbine generated 13.8 MW. The gain of 5.4 MW may be compared with the heat added from the biomass combustion, namely, 12.1 MWt. Thus, the biomass heat has a thermal efficiency of 44.7%, much higher than a typical simple biomass power plant.

New Zealand is another particularly favorable place since numerous large geothermal plants are surrounded by or close to forest plantations [20]. From among the many possible schemes that can capture these two sources of energy, here we show only two. Fig. 14.15 shows a biomass power plant that is boosted by a geothermal preheat in which the geosteam is superheated, which is a compound hybrid arrangement (See Section 14.5.3). Fig. 14.16 shows an integrated geothermal flash-binary plant where a biomass boiler provides superheat to the geothermal steam and includes two binary cycles, one heated by the separated geothermal brine and one by the back-pressure steam exhausted from the geothermal steam turbine.

Northern California has hosted a wood-waste/geothermal-preheat type power plant since 1989. The Honey Lake plant, located about 35 km east of Susanville in a sparsely populated area, is a 26.4 MW Rankine cycle unit that is fueled by wood waste. The low-pressure, low-temperature, plate-type feedwater heaters use hot geothermal fluid from a pair of wells in the Wendel geothermal field. A third well is used for reinjection.

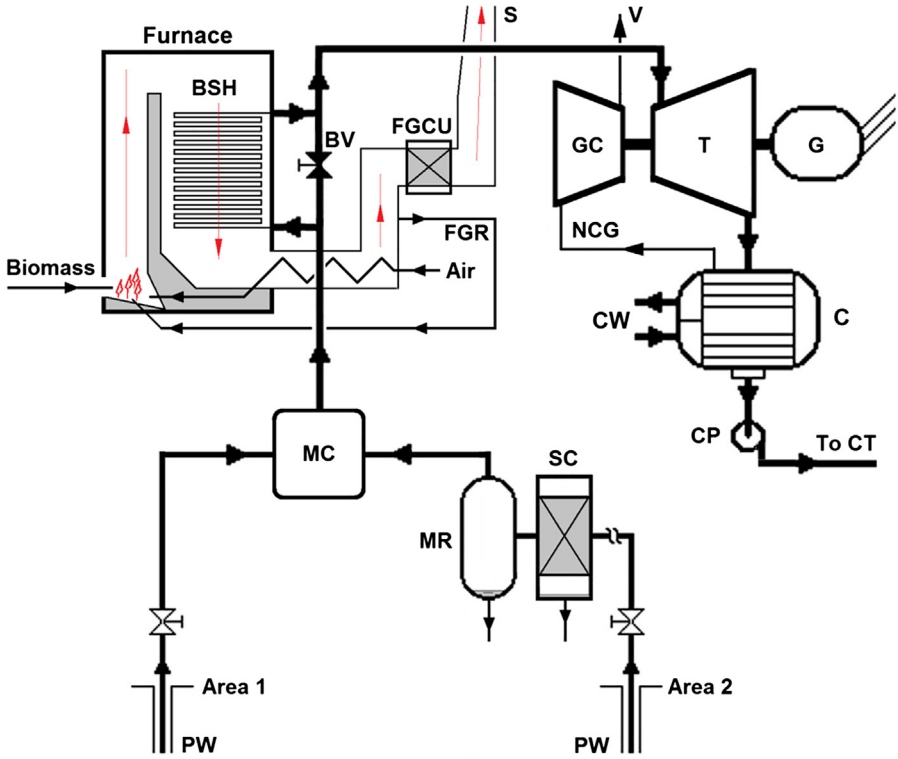

Figure 14.14 Cornia repowered dry-steam/biomass hybrid power plant [F. Lazzeri, Enel Green Power: Personal comm., May 15, 2015]; see Nomenclature.

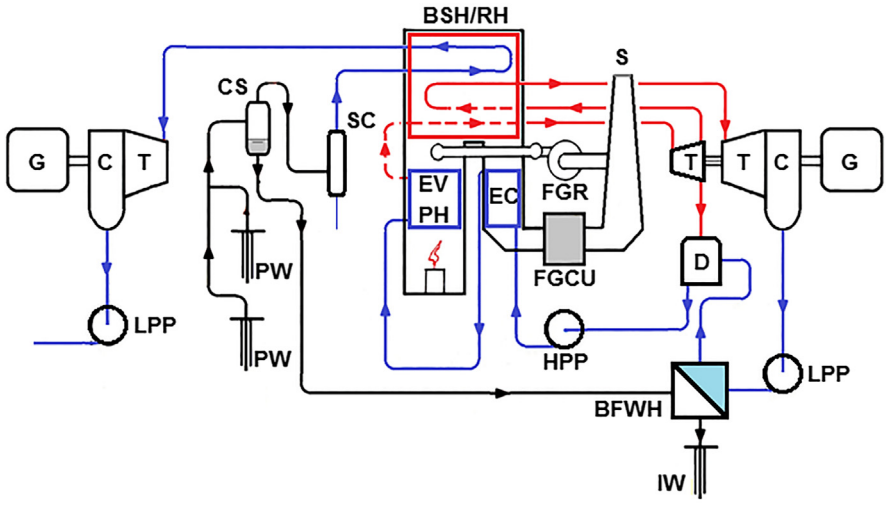

Figure 14.15 Compound hybrid geothermal wood-waste hybrid system [20]; see Nomenclature.

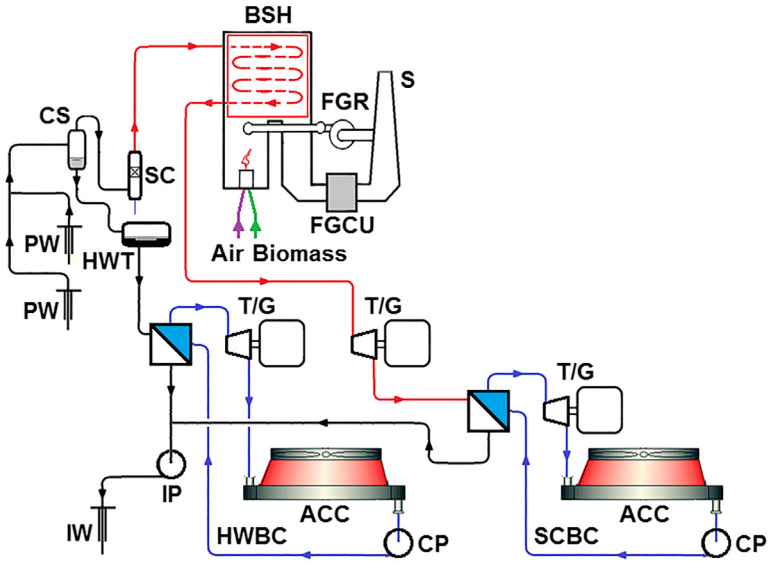

Figure 14.16 Integrated flash and binary geothermal power plant with a biomass superheater; see Nomenclature.

The thermal contribution from geothermal energy accounts for about 1.8 MW of electrical output. There is a solar PV system adjacent to the power plant, but it is not connected to the hybrid unit. [Pers. comm., Mr. Pat Holley, Greenleaf Power, December 19, 2023.]

14.5.6 Geopressure Thermal–Hydraulic Hybrid Systems

There are places where reasonably hot geofluids are found under very high pressures and with significant amounts of dissolved petroleum gases. One such region is the Gulf Coast of the United States. If these fluids can be safely brought to the surface via wells, it should be possible to utilize three different forms of energy contained within them. The high pressure can be used to drive a hydraulic turbine, the dissolved gases can be released, captured and either sold or burned on-site, and the thermal energy used to power a geothermal power plant is either flash or binary.

Fig. 14.17 shows one possible arrangement of a geopressured power plant in which the gas, assumed to be methane, is fed to a combustion chamber of a gas turbine after being separated from the exhaust section of a hydraulic turbine. The separated liquid is flashed to generate steam that is superheated by the gas turbine exhaust and then expanded in a steam turbine. Many variations on this basic design are possible [21]. Alternatively, a combustion engine may replace the gas turbine, a double-flash system may replace the single-flash, and a binary bottoming cycle may replace the steam turbine. Fig. 14.18 represents one such variation. The US Dept. of Energy built and

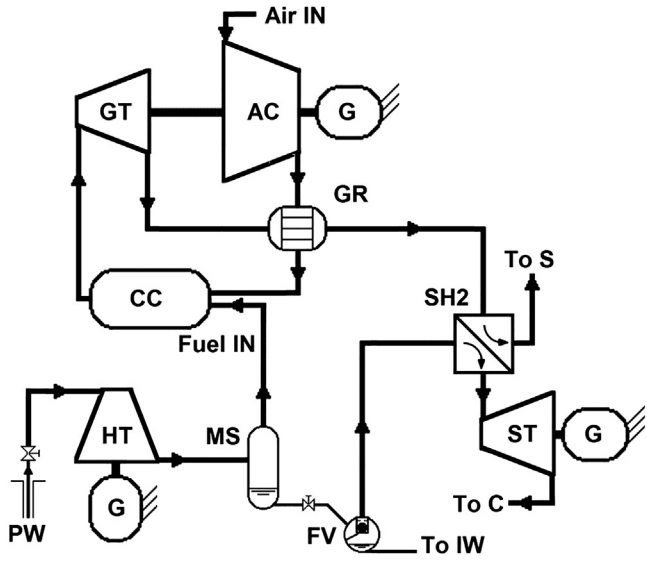

Figure 14.17 Geopressured thermal-hydraulic power system with gas turbine; see Nomenclature.

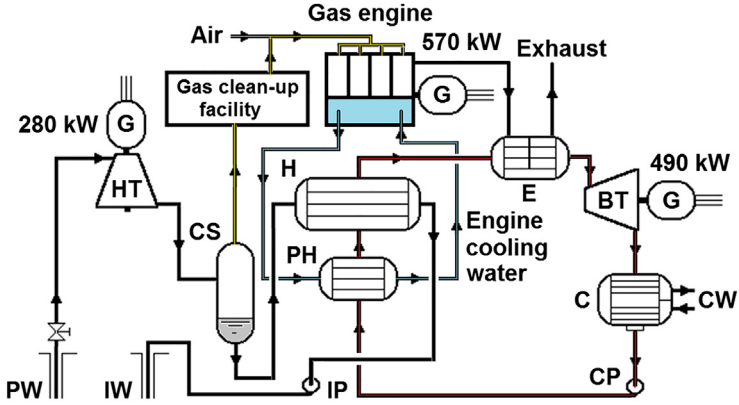

Figure 14.18 Geopressure thermal-hydraulic power system with reciprocating gas engine. Depending on the price of natural gas, the gas engine can be eliminated and the gas sold into a pipeline; see Nomenclature.

operated a pilot plant at Pleasant Bayou in Texas from 1989−90; the plant was modeled after Fig. 14.18 but without the hydraulic turbine [15].

Given the variable thermodynamic characteristics that the geopressured fluid may exhibit, a flexible suite of power system options is needed to exploit the resource. Additionally, the prices of electricity and gas will dictate which option is the thermo-economic optimum.

Writing in 1981, Khalifa [21] concluded that the levelized cost of electricity from hybrid geopressured plants in the Gulf Coast region would be about 40%–50% lower than electricity generated using conventional geothermal flash and binary plants, assuming realistic gas prices and cost escalators. Furthermore, the cost of electricity is strongly dependent on the methane content of the geofluids but only weakly dependent on the wellhead temperature. A more recent study [22] found that near-term conditions as of 2004 were not favorable for exploitation of geopressured resources for electric power.

14.6 Geothermal–Solar Hybrid Systems

The idea of using solar energy to enhance geothermal power plants has a long history [13]. Solar collectors may be used to heat geothermal steam or brines to temperatures greater than naturally available from the reservoir. Field experiments have shown that there are advantages from a thermodynamic standpoint. The most important practical consideration is the mismatch between availability of the intermittent solar component and the steady geothermal component. Without a commercial means of storing the solar energy for those periods when the sun is not shining, the geothermal plant must operate under two different modes, one of which will necessarily be nonoptimal. The other important factor is the economics of the hybrid system. Given the high specific capital cost of solar systems relative to geothermal ones, it usually takes special circumstances to justify the addition of a solar system to a geothermal power plant.

Process flow diagrams are presented in Section 14.6.1 for some hybrid systems that incorporate CSP systems with geothermal flash and binary plants. While PV systems have been installed at one geothermal plant, the Stillwater binary plant in Nevada, USA, the two energy sources are thermodynamically separate and thus achieve no synergy beyond sharing common infrastructure such as roads and transmission lines; see Section 14.6.2.

14.6.1 Geothermal–Concentrating Solar Power Hybrid Plants

A parabolic solar collector may be used to superheat the working fluid in a geothermal binary plant as shown schematically in Fig. 14.19. Since binary plants suffer from having a small temperature range across the power cycle, raising the upper temperature in this way will lead to higher thermal efficiency. However, the turbine must deal with saturated vapor when the solar loop is inactive. Thus, if the turbine is designed for superheated inlet conditions, it will perform off-design when the sun is not available or vice versa. A simple storage tank (ST) system is shown in the figure that allows for some hours of continued operation in hybrid mode after the sun sets, but when the hot fluid in the storage tank is depleted, the plant reverts to basic geothermal operation.

A geothermal double-flash plant offers several opportunities for enhancement from solar energy; see Fig. 14.20. The solar heat exchanger (SHX) is shown

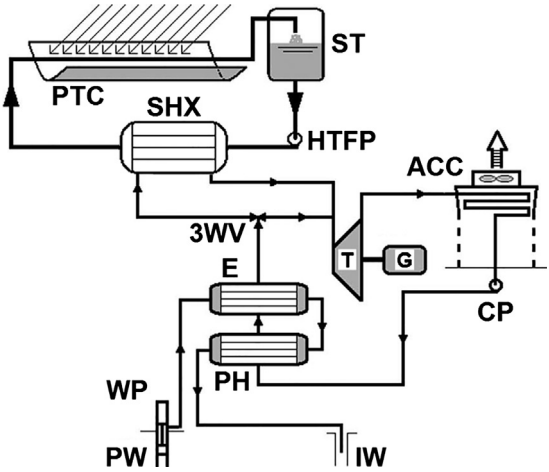

Figure 14.19 Hybrid geothermal-solar system with parabolic trough collector; see Nomenclature.

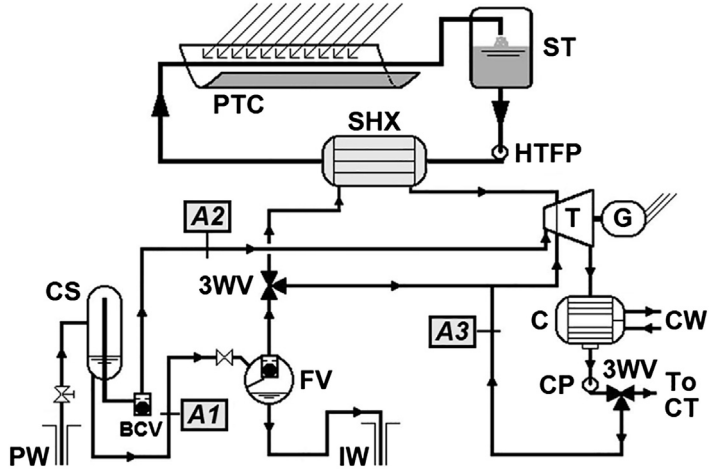

Figure 14.20 Possible configurations of geothermal flash plant augmented with parabolic trough collector; see Nomenclature.

superheating the low-pressure flashed steam before mixing with the steam leaving the first stages of the steam turbine. This will allow the first of the low-pressure stages to see superheated steam instead of wet steam, and to produce a drier expansion line and higher turbine efficiency. Three other options for locating the SHX are shown as *A1*, *A2,* and *A3*. *A1* would preheat the separated brine and allow the flash process to generate more steam; *A2* would superheat the separated steam from the cyclone separator for turbine entry; and *A3* would heat and evaporate a portion of the steam condensate for reuse in the LPT section. Recall that there is excess condensate

available from the water-cooling tower and this would tap into that excess. Field experiments of these systems have been conducted at the Ahuachapán geothermal plant with good results [23,24].

Recently, a proposal [25] has been put forth for a novel system at Cerro Prieto, near Mexicali, Mexico where there is abundant sunlight [G. Hiriart L., ENAL: Pers. comm., June 1, 2015]. Hiriart would like to rejuvenate the now-closed Cerro Prieto I power station by drilling new wells and installing down-hole pumps to produce high-pressure brine. The temperature would be fairly low, about 140°C, but would be raised to about 155°C by solar collectors during the day. Parabolic collectors would be used to heat a heat transfer medium (oil), as shown in Fig. 14.21, which in turn would impart heat to the brine in a simple tube-in-tube heat exchanger formed by the brine transmission pipeline. The plant would be an air-cooled binary in which the cycle working fluid would enter the turbine as an enhanced superheated vapor when the sun is shining but as essentially a saturated vapor otherwise. The incremental daytime power attributed to the solar input would serve to compensate for the poor heat transfer in the air-cooled condensers that limits power output owing to the hot ambient conditions. To date, this proposal has not been implemented.

In 2015 a CSP system was added to the Stillwater binary plant in Nevada, USA. The purpose is to raise the geofluid temperature after it is pumped to the surface, but before it enters the heat exchangers of the binary cycle. Over the years of operation, the geofluid temperature had declined and the new CSP system restores the plant to its designed geofluid temperature. Fig. 14.22, a highly simplified schematic, shows the design; a heat transfer fluid (pressurized water with a corrosion inhibitor) circulates between the solar collector (PTC) and the brine heat exchanger (HXER). The new CSP system costs about US $14.5M and is expected to add about 2 MWe of power and 3500 MWh of electricity annually to the Stillwater output [26].

14.6.2 Geothermal–Photovoltaic Hybrid Plants

One example of a PV–geothermal power plant is at the Stillwater plant in Nevada; see Figs. 14.23 and 14.24. Part of this PV system preceded the CSP system

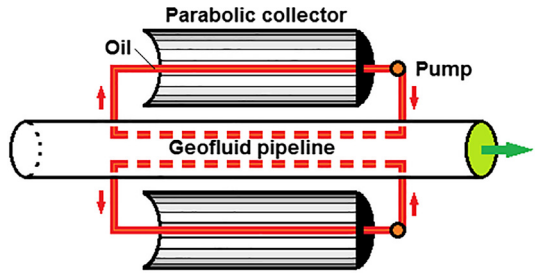

Figure 14.21 Means of superheating geothermal steam traveling from separators to the turbine at Cerro Prieto, Mexico.
After Ref. [25].

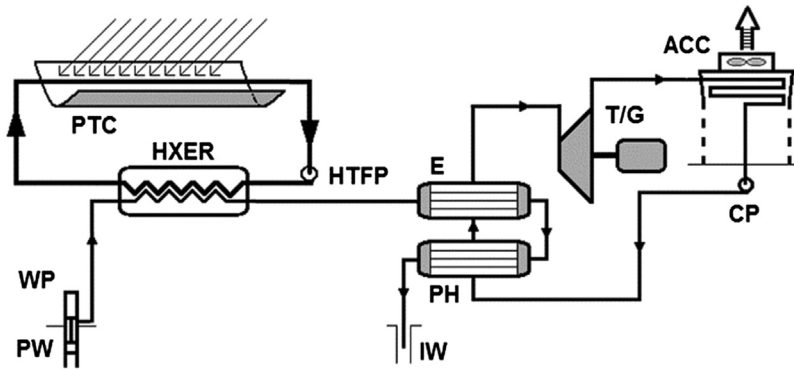

Figure 14.22 Flow diagram for Stillwater CSP-geothermal binary power plant [26]; see Nomenclature.

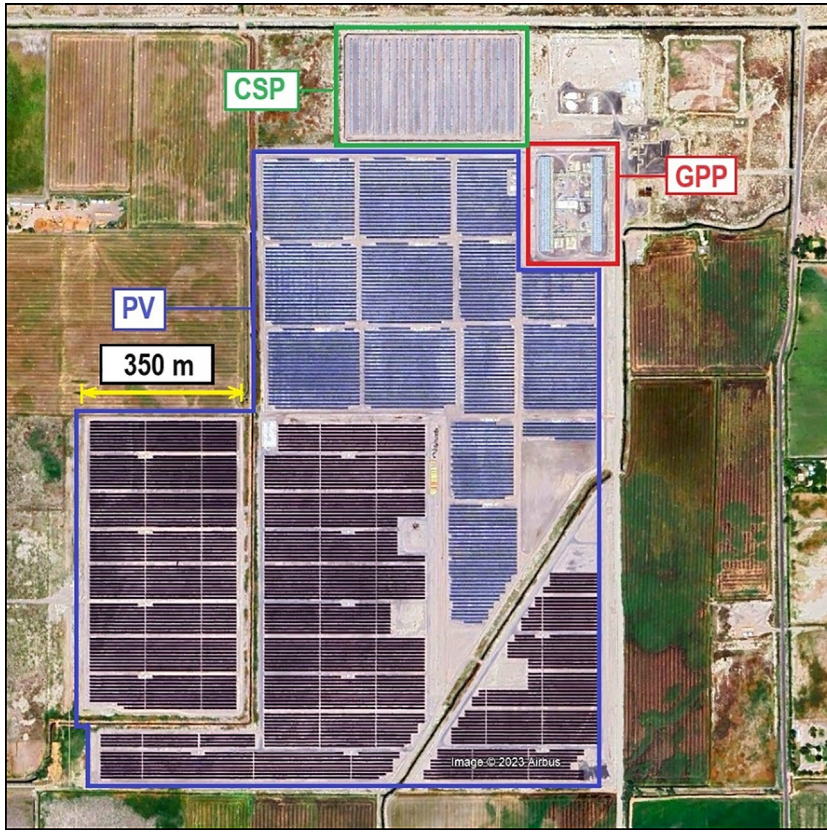

Figure 14.23 Aerial view of Stillwater power plant with adjacent concentrating solar power and photovoltaic (PV) systems. The darker sections of the PV field at the lower left and right are dedicated to fulfilling a 27 MW power purchase agreement between the plant owner, Enel Green Power NA, and Wynn Las Vegas Resorts [28]. The other PV panels were the original ones used to supplement the output of the geothermal plant.
Modified Google Earth image, August 18, 2023.

Figure 14.24 View of Stillwater binary plant showing a few of the 89,000 polycrystalline panels in the original PV system.
Courtesy of Author, July 29, 2012.

described above. The geothermal binary plant has an installed capacity of 47.2 MW but has not achieved that level of output in practice owing to insufficient supply of geofluid from the production wells, lower than expected geofluid temperature, and insufficient reinjection capacity despite the drilling of wells to boost performance. In 2022, the geothermal plant operated at a capacity factor of 38.3% (gross) and 22.9% (net) [27]. The shortfall in the contracted power that the owner is obligated to deliver to the grid is offset using a 26 MW (peak) portion of the PV system. This is particularly attractive economically, as the price of electricity is highest during hot summer days when sunshine is plentiful at the site. Geothermal and PV plants share a common infrastructure but do not interact in any thermodynamically synergistic manner.

Two other geothermal plants in Nevada employ solar PV plants to supplement the geothermal power: Patua (see Fig. 14.25) and Tungsten Mountain. Patua is a 3×16 MW or 48 MW binary plant that is operating below its installed capacity, for example, at a net capacity factor of 23.6% in 2022. The PV array adds 14.5 MW (peak) solar capacity. Tungsten Mountain is a 37 MW (installed) binary plant with a 7 MW (peak) solar PV system. In 2022, this plant operated at a net capacity factor of 90.0% [27].

Türkiye, which has recently seen exponential growth in geothermal power installations [29], also is combining solar PV with some of the geothermal plants already in operation. The 45 MW Alaşehir-1 JES flash plant in Manisa Province was recently augmented by a 3.75 MW (peak) solar PV plant; see Fig. 14.26. The solar array

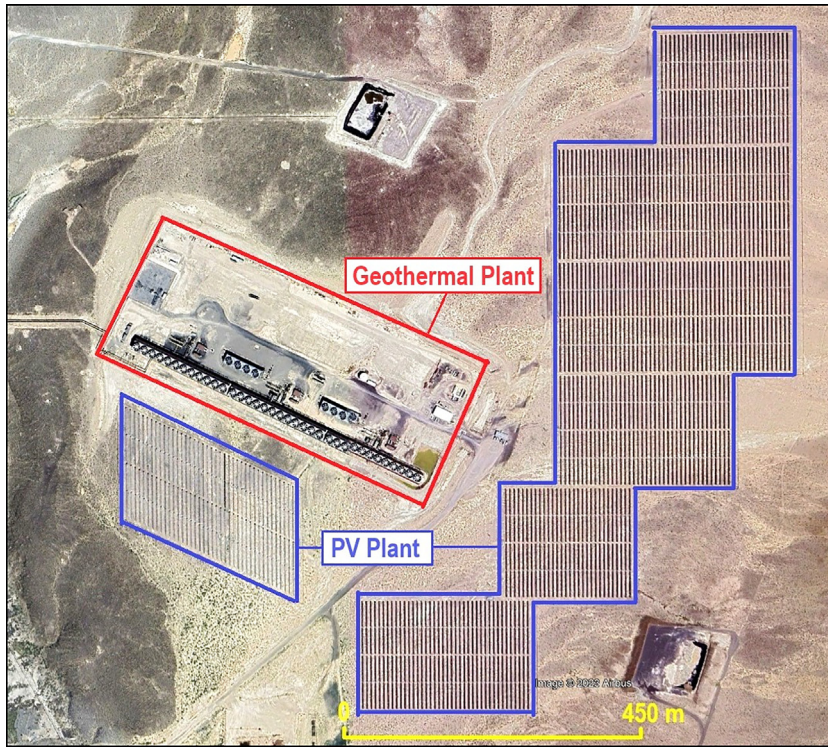

Figure 14.25 Aerial view of Patua 48 MW (installed) power plant with adjacent 14.5 MW (peak) PV field.
Modified Google Earth image, August 23, 2023.

consists of 31,200 thin-film panels each rated at 115 W (peak) and covers 6.2 ha of land [30]. The electricity so generated helps cover the parasitic power loads of the geothermal plant. In planning are two other hybridizations, the Kızıldere 2 (10 MW solar) [31] and Kızıldere 3 (21 MW solar) [32] geothermal flash power plants also owned by Zorlu. Once again, the objective is to cover the plant's internal power needs and increase the net power for sale.

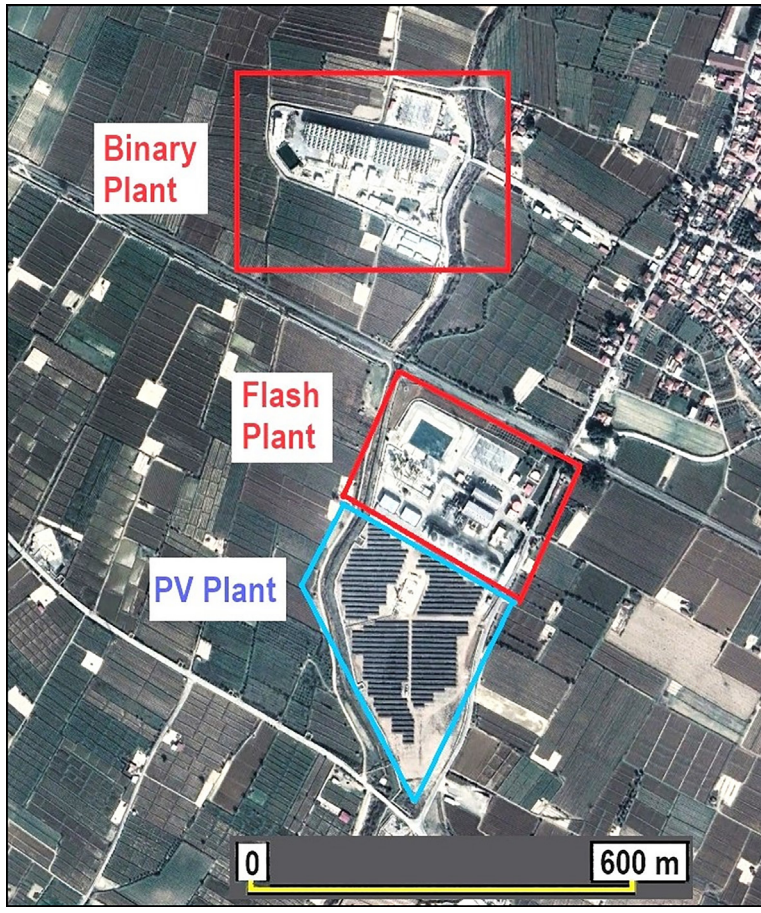

Figure 14.26 Aerial view of Ataşehir power plants. The 3.75 MW PV plant is associated with the 45 MW geothermal flash plant.

14.7 Conclusions

This chapter has shown that hybrid power plants involving geothermal and other energy sources can be designed and built in a wide variety of ways. Combined geothermal plants of many types are routinely constructed, and several examples are described herein. Generally, the goal of these hybrid and combined systems is to achieve some form of synergy, that is, to produce more power by combining two

sources of energy or power systems cleverly and thereby obtain more output than could be achieved using two separate SOTA power plants. The thermodynamic conditions required to achieve this are described for several types of plants. Some successful plants are presented to demonstrate how effective these plants can be. However, the feasibility of hybrid plants turns on many site-specific factors that must be favorable for success, including colocation of the energy sources, prices of energy and electricity, assured availability of energy supplies, environmental permitting, and meeting all regulatory requirements.

Nomenclature

3WV	three-way valve
AC	air compressor
ACC	air-cooled condenser
BCV	ball check valve
BFP	boiler feed pump
BFWH	brine feedwater heater
BHT	brine holding tank
BSH	biomass superheater
BT	binary turbine
BV	bypass valve
C	condenser
CC	combustion chamber
CP	condensate pump
CS	cyclone separator
CSP	concentrating solar power
CT	cooling tower
CW	cooling water
D, DA	deaerator
E, EV	evaporator
EC	economizer
F, FV	flasher, fossil (Fig. 14.1), flash vessel
FGCU	flue gas cleanup
FGR	flue gas recirculator
FSH	fossil superheater
FWH	feedwater heater
FWP	feedwater pump
G	generator, geothermal (Fig. 14.1)
GC	gas compressor
GFWH	geothermal feedwater heater
GR	geothermal recuperator
GST	geothermal steam turbine
GT	gas turbine
H	heater, hybrid (Fig. 14.1)

HPP, LPP	high-, low-pressure pump
HPS, MPS, LPS	high-, medium-, low-pressure separator
HPST, LPST	high-, low-pressure steam turbine
HPT, IPT, LPT	high-, intermediate-, low-pressure turbine
HT	hydraulic turbine
HTFP	heat transfer fluid pump
HWBC	hot water binary cycle
HWT	hot water tank
HXER	heat exchanger
IP	injection pump
IW	injection well
MC	mixing chamber
MR	moisture remover
MS	methane separator
NCG	noncondensable gas
OP	orifice plate
PH	preheater
PTC	parabolic trough collector
PV	photovoltaic
PW	production well
R	recuperator
RH	reheater
S	stack, solar (Fig. 14.1)
SC	scrubber
SCBC	steam condensed binary cycle
SG	steam generator
SH	superheater
SHX	solar heat exchanger
SR	steam recuperator
ST	steam turbine; storage tank
T/G	turbine/generator
WP	well pump

References

[1] Janes J, Shurley LA, White L, Deter ER. Evaluation of a superheater enhanced geothermal steam power plant in the Geysers area: final report. Sacramento, CA: California Energy Commission; June 1984. Rep. No. P700-84-003.

[2] DiPippo R. An analysis of an early hybrid fossil-geothermal power plant proposal. Geotherm Energy Mag 1978;6:31−6.

[3] Kestin J, DiPippo R, Khalifa HE. Hybrid geothermal-fossil power plants. Mech Eng 1978; 100:28−35.

[4] Khalifa HE, DiPippo R, Kestin J. Hybrid fossil-geothermal power plants. In: Proceedings of the 5th energy technology conference; 1978. p. 960−70. Washington, DC.

[5] Khalifa HE, DiPippo R, Kestin J. Geothermal preheating in fossil-fired steam power plants. In: Proceedings of the 13th intersociety energy conversion engineering conference. 2; 1978. p. 1068−73.

[6] DiPippo R, Khalifa HE, Correia RJ, Kestin J. Fossil superheating in geothermal steam power plants. Geotherm Energy Mag 1979;7:17−23.
[7] DiPippo R, Avelar EM. Compound hybrid geothermal-fossil power plants. Trans Geoth Resour Counc 1979;3:165−8.
[8] DiPippo R. Impact of hybrid combustion-geothermal power plants on the next generation of geothermal power systems. In: Proceedings of the third annual geothermal conference and workshop. Electric Power Research Institute; 1979. pp. 6.1-6.6.
[9] Khalifa HE. Hybrid fossil-geothermal systems. Sect. 4.3. In: Kestin J, DiPippo R, Khalifa HE, Ryley DJ, editors. Sourcebook on the production of electricity from geothermal energy. U.S. Department of Energy, U.S. Government Printing Office; 1980.
[10] DiPippo R, DiPippo EM, Kestin J, Khalifa HE. Compound hybrid geothermal-fossil power plants: thermodynamic analyses and site-specific applications. Trans ASME J Eng Power 1981;103:797−804.
[11] Khalifa HE. Gas-turbine-topped hybrid power plants for the utilization of geopressured geothermal resources. ASME Paper No. 81-Pet-5. In: Proceedings of the energy-sources technology Conference and exhibition; 1981.
[12] The Ralph M. Parsons Company. System design verification of a hybrid geothermal/coal fired power plant. September 1978. Project No. 5805.
[13] Hiriart L.B G, Gutierrez N LCA. Calor del Subsuelo para Generar Electricidad − Combinacion Solar-Geothermia. Heat from the Earth to generate electricity− combined solar-geothermal, vol 313. Ingenieria Civil; 1995. p. 13−22.
[14] Moya R. P, DiPippo R. Miravalles unit 5 bottoming binary plant: planning, design, performance and impact. Geothermics 2007;36:63−96.
[15] DiPippo R. Geothermal power plants. In: Principles, applications, case studies and environmental impact. 3rd. Oxford, England: Butterworth-Heinemann: Elsevier; 2012.
[16] James J. Evaluation of a superheater enhanced geothermal steam power plant in the Geysers area. Rep. P700-84-003. California Energy Commission, Siting and Environmental Division; 1984.
[17] National Institute of Standards and Technology (NIST). Reference Fluid Thermodynamic and Transport Properties. U.S. Department of Commerce. http://www.nist.gov/srd/nist23.cfm.
[18] U.S. Energy Research and Development Administration (ERDA). Site-specific analysis of hybrid geothermal/fossil power plants; 1977. Division of Geothermal Energy, Prime Contractor−City of Burbank.
[19] The Ralph M. Parsons Company. System design verification of a hybrid geothermal/coal fired power plant. Prime Contractor − City of Burbank; September 1978. Project No. 5805.
[20] Thain I, DiPippo R. Hybrid geothermal-biomass power plants: applications, designs and performance analysis. In: Proceedings of the world geothermal Congress 2015, Melbourne, Australia; April 2015.
[21] Khalifa HE. Hybrid power plants for geopressured resources. EPRI Project RP 1671-2, United Technologies Research Center; June 22, 1981.
[22] Griggs J. A re-evaluation of geopressured-geothermal aquifers as an energy resource. Masters Thesis. Louisiana State University, Craft and Hawkins Department of Petroleum Engineering; August 2004.
[23] Handel S, Alvarenga Y, Recinos M. Geothermal steam production by solar energy. Trans Geoth Resour Counc 2007;31:503−10.
[24] Alvarenga Y, Handel S, Recinos M. Solar steam booster in the Ahuachapán geothermal field. Trans Geoth Resour Counc 2008;32:395−9.

[25] Hiriart L G. Complejo Híbrido de Energías Renovables con Planta de Almacenamiento en la Frontera Norte. Hybrid renewable energy plant with storage at the North Border. Mexico: Academia de Ingeniería A.C.; March 26, 2015 [in Spanish].
[26] DiPippo R. Geothermal power plants. In: Principles, applications, case studies and environmental impact. 4th. Oxford, England: Butterworth-Heinemann: Elsevier; 2015.
[27] Jowitt SM, Micander R, Richards M, Reynolds D. The Nevada mineral industry 2022. Nevada Bureau of mines and geology. Special Publication; 2023. MI-2022.
[28] Enel. Enel sells solar energy from new 27 MW plant in USA to Wynn Las Vegas resort. January 25, 2018. https://www.enelgreenpower.com/media/press/2018/1/enel-sells-solar-energy-from-new-27-mw-plant-in-usa-to-wynn-las-vegas-resort.
[29] Serpen U, DiPippo R. Turkey—a geothermal success story, A retrospective and prospective assessment. Geothermics 2022;101:102370.
[30] Cariaga C. Zorlu Energy commissions first hybrid power plant in Ataşehir, Türkiye. ThinkGeoEnergy; April 12, 2023. https://www.thinkgeoenergy.com/zorlu-energy-commissions-first-hybrid-power-plant-in-alasehir-turkiye/.
[31] Cariaga C. Zorlu Energy planning to invest on hybrid power plant. ThinkGeoEnergy; May 26, 2023. https://www.thinkgeoenergy.com/zorlu-energy-planning-to-invest-on-hybrid-power-plant/.
[32] Cariaga C. Kızıldere 3 capacity increases with reclassification as solar-geothermal hybrid plant. ThinkGeoEnergy; March 29, 2023. https://www.thinkgeoenergy.com/kizildere-3-capacity-increases-with-reclassification-as-solar-geothermal-hybrid-plant/.

Further reading

DiPippo R. Geothermal power plants. In: Ali S, editor. Comprehensive renewable energy, vol 7. Oxford, England: Elsevier; 2012. p. 207−37.
Lentz I, Almanza R. Geothermal-solar hybrid system in order to increase the steam flow for geothermic cycle in Cerro Prieto, Mexico. Trans Geoth Resour Counc 2003;27:543−6.
Lentz I, Almanza R. Solar−geothermal hybrid system. Appl Therm Eng 2006;26:1537−44.
Lentz I, Almanza R. Parabolic troughs to increase the geothermal wells flow enthalpy. Sol Energy 2006;80:1290−5.
Manente G, Field R, DiPippo R, W Tester J, Paci M, Rossi N. Hybrid solar-geothermal power generation to increase the energy production from a binary geothermal plant. Paper No. IMECE 2011-63665. In: Proceedings of the 2011 ASME international mechanical engineering congress and exposition. Denver, Colorado: ASME; 2011.